Supramolecular Assemblies of Trimesic Acid on a Cu(100) Surface

A. Dmitriev,*,† N. Lin,† J. Weckesser,† J. V. Barth,‡ and K. Kern†,‡

Max-Planck-Institut für Festkörperforschung, D-70569 Stuttgart, Germany, and Institut de Physique des Nanostructures (IPN), Ecole Polytechnique Fédérale de Lausanne, CH-1015 Lausanne, Switzerland

Received: November 15, 2001; In Final Form: February 21, 2002

The adsorption and supramolecular ordering of trimesic acid (TMA), 1,3,5-benzenetricarboxylic acid $C_6H_3(COOH)_3$, on a Cu(100) surface has been studied in-situ in ultrahigh vacuum by variable-temperature scanning tunneling microscopy. We have elucidated the real-space structures of distinct self-assembled supramolecular aggregates at the molecular scale. At low temperatures (∼200 K), two-dimensional networks evolve. They reflect extensive hydrogen-bond formation of a flat-lying species, similar to supramolecular ordering in the bulk TMA crystal structure. At room temperature, more densely packed stripe arrangements form. They are associated with a bonding transition leading to an upright geometry due to carboxylate formation.

1. Introduction

Self-assembly provides unique routes to obtain nanoscale supramolecular structures, i.e., highly organized and extended molecular architectures which are stabilized by noncovalent bonds.[1−4] Recent studies, where an experimental technique − predominantly scanning tunneling microscopy (STM) − was employed, revealed that at well-defined surfaces direct insight into self-assembly phenomena in two dimensions can be gained.[5−11] Systematic investigations in this field may eventually lead to recipes for the deliberate construction of supramolecular architectures and the positioning of functional units in specific geometries, which are expected to be of value in novel technological applications at the nanoscale, such as molecular electronics devices.[12−14]

A promising class of candidates to form supramolecular aggregates are molecular species comprising functional groups for hydrogen bond formation, which provide the possibility of benefiting from the H-bond energetics and directionality to fabricate highly organized assemblies.[15] Such species have been employed at surfaces,[5,8,9,11] and the results demonstrate the successful use of organic molecules, e.g., with moieties for head-to-tail or lateral coupling, and suggest that in general species with functional groups providing geometrical (steric) or electronic complementarity can be employed.

The molecule trimesic acid (TMA, 1,3,5-benzenetricarboxylic acid, $C_6H_3(COOH)_3$) represents a prototype material for supramolecular self-assemblies.[16−19] As shown in Figure 1a, it is a polyfunctional carboxylic acid with 3-fold symmetry comprising a phenyl ring and three identical carboxyl endgroups in the same plane. TMA is known to assemble in diverse supramolecular structures due to the trigonal exodentate functionality, and the most common motif identified therein is a planar honeycomb network structure formed through the dimerization of carboxyl groups, as depicted in Figure 1b. In the three-dimensional (3D) α-polymorph of the TMA crystal structure, these networks interpenetrate, i.e., the ≈14 Å diameter holes of the honeycombs are catenated. Moreover, the tendency of network formation in

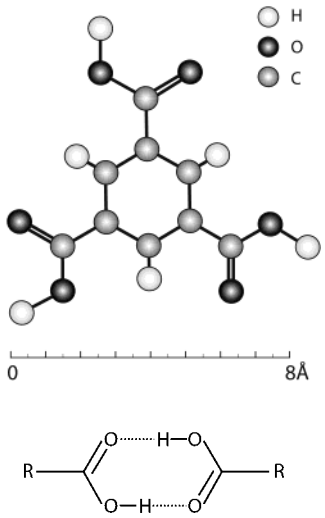

Figure 1. (a) Molecular structure of trimesic acid. (b) Hydrogen-bond mediated dimerization of the self-complementary carboxyl groups.

TMA is frequently employed for the fabrication of clathrates (inclusion complexes).[17−20]

The ordering principles of trimesic acid upon confinement to two dimensions thus represent an exemplary model system in the understanding of supramolecular self-assembly at surfaces. To tackle this issue, we have performed variable-temperature STM investigations on the adsorption and supramolecular ordering of TMA on a Cu(100) substrate. Our results reveal that at low temperatures (<280 K), flat-lying TMA molecules form islands where the honeycomb motif prevails, similar to that identified in 3D supramolecular structures. This demonstrates that 3D ordering principles from organic crystals can be translated to the 2D scene. However, due to the chemical activity of the Cu surface atoms, the low-temperature arrangements irreversibly transform to stripe-shaped supramolecular structures at higher substrate temperatures (∼300 K). This is associated with a deprotonation of the molecules, leading to carboxylate formation and an upright bonding geometry. The results demonstrate how the adsorbate−substrate interaction can be exploited to drive the transformation of supramolecular arrangements at surfaces.

* E-mail: a.dmitriev@fkf.mpg.de.
† Max-Planck-Institut für Festkörperforschung.
‡ Ecole Polytechnique Fédérale de Lausanne.

10.1021/jp014214u CCC: $22.00
Published on Web 06/19/2002

2. Experimental Section

The sample preparation and characterization have been conducted in an ultrahigh vacuum (UHV) environment, providing well-defined conditions for the experiment. The UHV system (base pressure $\sim 3 \cdot 10^{-10}$ mbar) is equipped with a home-built variable-temperature UHV−STM described elsewhere (operational in the range of 40−800 K),[21] as well as standard facilities for sample preparation and a quadrupole mass spectrometry analysis (QMS). The Cu(100) surface was cleaned by repeated cycles of Ar^+ sputtering and subsequent annealing (500 eV, 6 mA, 800 K), allowing atomically flat terraces of up to 200 nm width separated by monatomic steps to be obtained. The STM experiments were performed in the constant current mode, with maximum bias voltages up to 2 V. Data were obtained starting in the temperature range 180−300 K. Commercially available TMA (Fluka Chemie AG) in powder form was deposited by organic molecular beam epitaxy (OMBE) from a Knudsen-cell type evaporator. The temperature of the cell was constantly held at 460 K during the evaporation since decomposition of TMA molecules can occur at around 520 K. QMS spectra of the molecular beam reveal accordingly the characteristic peak of nondissociated TMA molecules at 193 amu (according to the NIST Mass Spectrometry Data[22]). Deposition rates were calibrated using area estimation from the STM images at monolayer coverages (according to 200 • 200 Å STM topograph, performed at 300 K, at 1 ML one adsorbed TMA molecule corresponds to 22 Cu surface atoms).

3. Results and Discussion

3.1. The Low-Temperature Phase with the Two-Dimensional Honeycomb Motif. The low-temperature phase of TMA was prepared with the temperature of the substrate held in the range 192−280 K for different experimental sets. In Figure 2a, an exemplary STM image (taken at 205 K) of self-assembled TMA aggregates is depicted. In this experiment, the deposition took place at 240 K, and subsequently, the crystal was cooled to the imaging temperature. In the insets, the atomically resolved clean Cu(100) surface revealing the orientation of the high-symmetry [011] direction and a close view of the supramolecular structure are shown. The triangular appearance of the molecules with a characteristic side length of ≈8 Å (which agrees with the dimensions of an individual TMA molecule[23]) strongly suggests a flat-lying adsorption geometry; i.e., molecules are oriented with their phenyl rings parallel to the substrate (cf. the molecular geometry of TMA in Figure 1a). At low molecular coverages (in our experiments, TMA up to 0.1 ML were studied), physically adsorbed π-systems are preferentially oriented parallel to the metal surface, which is associated with π-bonding to the substrate.[24−27] In the case of TMA, the planar adsorption geometry is reflected in the molecules' apparent height of ∼1.5 Å in the STM images (cf. the STM contour line in Figure 2d), which is a typical value for planar aromatic molecules with a π-system oriented parallel to the surface.[28−30]

The data in Figure 2 reveal moreover that TMA islands with smooth borders have formed at the surface decorating the atomic steps. This implies a preferred TMA adsorption at the step edges and an appreciable low-temperature diffusion rate, which allows TMA molecules to transport at the substrate (only for temperatures below 200 K is the mobility suppressed such that only randomly scattered molecules could be observed). Furthermore, there must be edge mobility along island perimeters; otherwise the formation of fractal islands derived from a diffusion-limited aggregation scenario would be expected. Within the islands, a honeycomb motif with a periodicity of ≈20 Å prevails. This configuration (cf. the detailed view in the inset of Figure 2a) is associated with supramolecular self-assembly through dimerization of carboxyl endgroups, similar to the network structures in 3D TMA crystals. However, the hexagonally arranged mesh of TMA molecules is slightly distorted with respect to the honeycomb structure in bulk TMA crystal, and two equivalent, but rotated by 90° in respect to the Cu(100) azimuths, meshes can be distinguished (compare the configurations in Figure 2b and the inset therein). The distorted honeycomb structural motif of TMA has TMA−TMA distances through the mesh center of 20.4 Å ($8a_0$) and 22.8 Å ($8.94a_0$) (shown in the corresponding cross-sectional profiles of Figure 2c). The distortion is ascribed to the preferred adsorption of the molecules on a surface with corrugated potential energy. Preliminary results of ab initio calculations employing density functional theory with the generalized gradient approximation indicate that the molecules are preferentially bound at the 4-fold hollow site of the substrate and that bonding at top sites is unlikely (the energy difference is ∼0.2 eV; three layers of Cu(001) with a (5 • 5) unit cell were used).[31] This is a typical finding for adsorption of large organic molecules at metal surfaces and is in agreement with the fact that at temperatures below 160 K the adsorbed TMA molecules do not diffuse at the surface upon adsorption. To fulfill the requirement of the 4-fold hollow site adsorption on Cu(100) surface, a structural model for the distorted honeycomb motif is proposed in Figure 2d, which agrees with the STM data very well.

In the crystal structure of bulk α-polymorph trimesic acid, 14 Å diameter holes of the honeycomb exist,[16] implying the TMA−TMA distance of 19.7 Å through the mesh center and the OH···O bond length of 2.7 Å. With the present system, the TMA−TMA distances through the mesh center are 20.4 and 22.8 Å, giving rise to the average length of the OH···O bond close to 3.7 Å, which exceeds by ∼1 Å the corresponding distance in the crystalline α-phase of TMA.[16] Similarly increased hydrogen bond lengths have been reported with other systems, where COH···N bonding in supramolecular aggregates with 4-[*trans*-2-(pyrid-4-yl-vinyl)]benzoic acid at a Ag(111) surface was investigated.[9] They are associated with the occupation of high-symmetry positions at the substrate and moreover possibly reflect H-bond relaxation in the presence of the electron gas at the metal surface. The proposed supramolecular self-assembled configuration can thus be understood from the balance of two main factors: the TMA molecular geometry driving carboxyl group dimerization and the molecular π-orbital interaction with the copper surface, which suggests the most energetically favorable adsorption with the phenyl ring in the hollow site of the substrate. Note that for the network formation it must be assumed that within a single carboxyl group the H atom is free to transfer from one oxygen atom to the other in the adsorbed state, a behavior which is well-known for related systems.[32] In the absence of this effect, eight different configurations for flat-lying TMA would exist.

Albeit the data in Figure 2 clearly demonstrate that honeycomb structure prevails in the small islands, typically 20 nm by 20 nm in size, it was not possible to obtain a full layer or at least a large domain consisting exclusively of this structure. In particular, close-packed TMA arrangements coexist with the honeycomb structures, as shown in the inset on Figure 2b. In addition, pentagonal meshes, comprising five TMA molecules (which points out the absence of azimuthal alignment of individual molecules within these structures) are frequently found. The attempts to resolve superstructure patterns in LEED measurements were not successful. This lack of a long-range

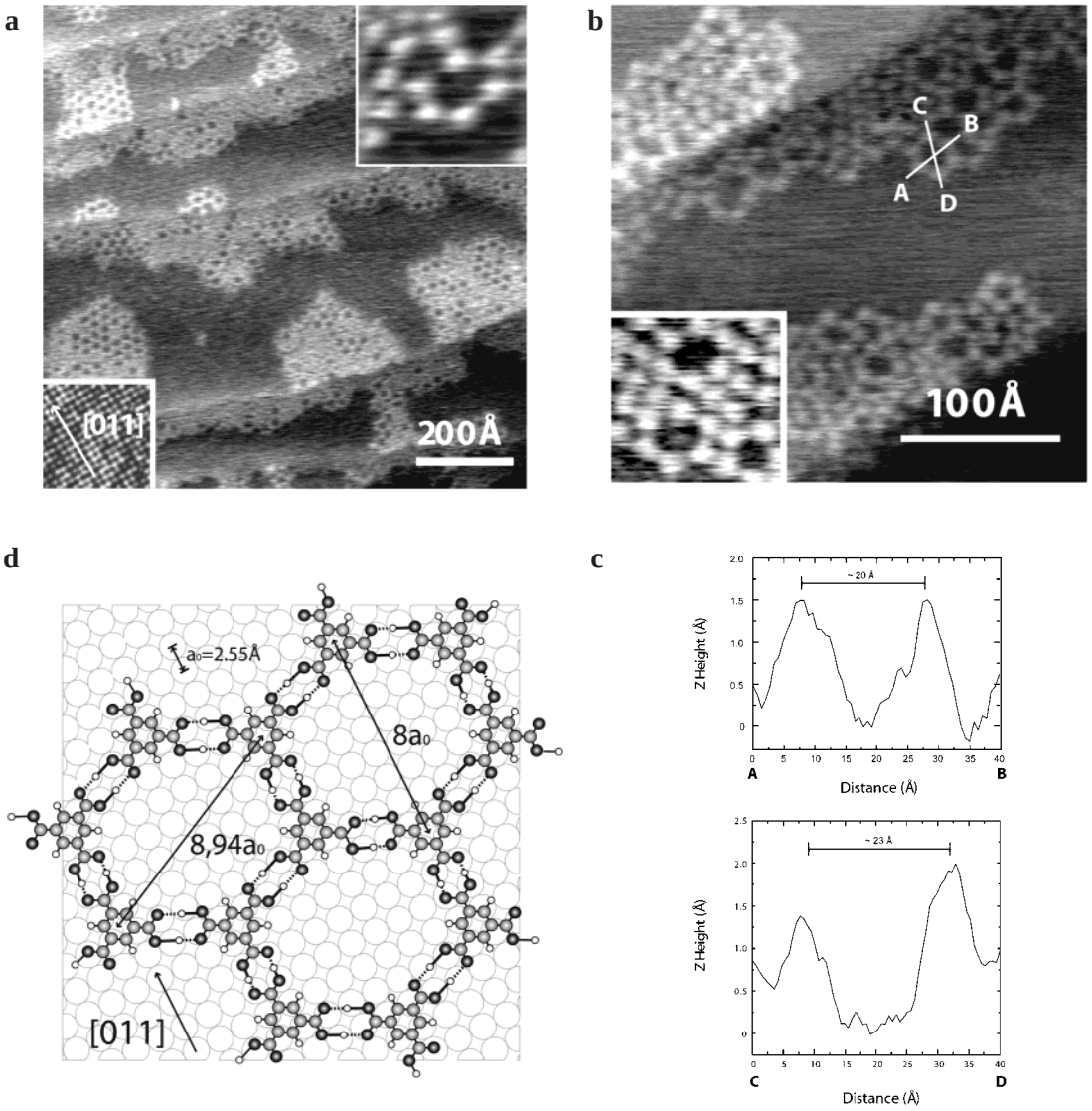

Figure 2. Low-temperature phase of TMA. (a) STM image of compact TMA islands at Cu(100) decorating atomic steps. ($100 \cdot 100$ nm^2, deposited on 240 K Cu (100), image taken at 205 K, bias voltage $U_b = 0.39$ V, tunneling current $I_t = 1.11$ nA). In the islands, a honeycomb motif is resolved which is associated with extensively hydrogen-bonded two-dimensional TMA networks. Insets: atomically resolved Cu (100) surface (lower left) and two meshes of the honeycomb structure (upper right). (b) STM image of honeycomb elements ($30 \cdot 30$ nm^2, $U_b = 0.511$V, $I_t = 0.139$ nA) with the corresponding height profiles (with lateral and height calibration performed) along the lines marked A−B and C−D are shown in the left- and right-hand sides, respectively, of part c. Inset in part b shows 90° rotated honeycomb meshes, coexisting with close-packed TMA molecules. (d) Structural model for the honeycomb network with individual TMA centered at substrate hollow sites. Oxygen atoms are represented by dark circles, carbon atoms by light gray circles, and hydrogen atoms by white ones. The characteristic dimensions of the structure are indicated.

order is believed to be associated with kinetic limitations and an appreciable substrate corrugation experienced by the adsorbed TMA. Efforts for equilibration to induce long-range order by increasing the substrate temperature destabilized the low-temperature phase, and the honeycomb networks were irreversibly transformed and cooling again does not lead to a restoration of the initial situation. Our STM observations reveal that with increasing temperatures the TMA honeycomb networks transform to a new regular phase at room temperature.

3.2. Room Temperature Phase: Stripe Structure. The room temperature phase can either be obtained upon annealing the low-temperature phase or directly upon molecular deposition with the substrate held at 300 K. Corresponding STM data are presented in Figure 3. One can clearly distinguish elongated striped islands in four distinct orientations, i.e., along the [0 3 $\bar{1}$], [0 $\bar{1}$ 3], [0 $\bar{1}$ 3], and [0 3 1] crystallographic directions (cf. the atomic resolution inset in Figure 3a for the high-symmetry directions of the pristine surface). This fact signals more pronounced adsorbate−substrate interaction as compared to the case of the low-temperature phase.

In the areas surrounding the islands, in the STM data at room temperature, frequent spikes and dashes appear in single scanlines. Such findings are typical for isolated mobile adsorbates with hopping rates comparable to the x-scanning frequency (in our case, typically ∼4 Hz).[33] A detailed analysis of the TMA surface diffusion was not performed. The observations demonstrate that at room temperature the surface is actually covered by a 2D crystalline phase (i.e., the islands) coexisting with a lattice gas. Only when TMA condensates in islands are the individual molecules at rest and they can be entirely imaged by STM due to the intermolecular lateral attraction.

Upon detailed inspection of the stripe phase, further features become apparent. This is demonstrated by the STM image in Figure 3b, where a high-resolution image of a [013]-oriented island is presented. First, it can be seen that intermolecular distances (measured as a distance between the maxima of the

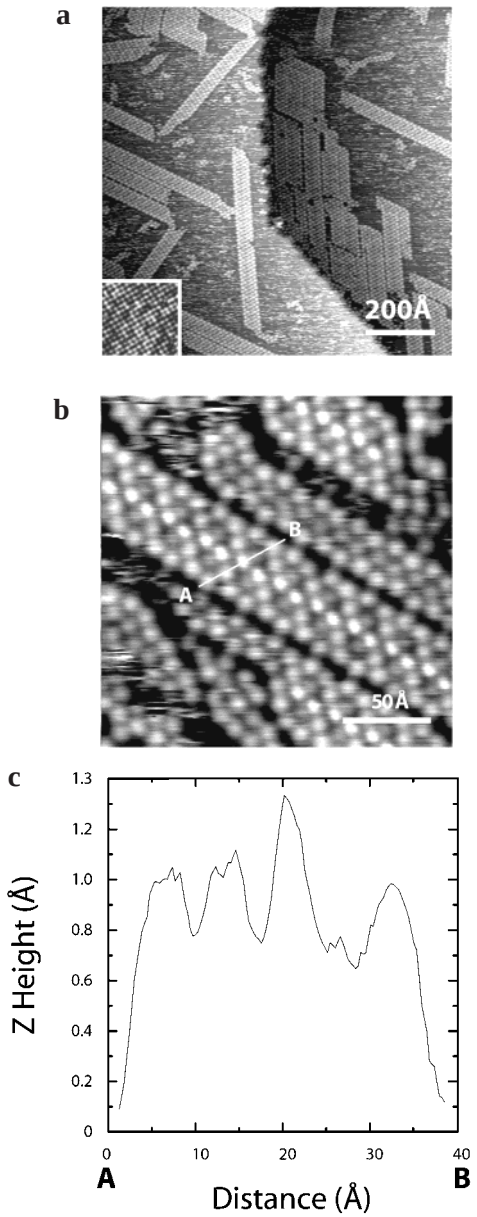

Figure 3. TMA/Cu(100) stripe phase evolving at room temperature. (a) STM image taken shortly after deposition at room temperature (100 · 100 nm^2, $U_b = 0.752$ V, $I_t = 0.54$ nA). Four distinct orientations of the islands can be seen (inset: atomically resolved pristine Cu(100) surface). (b) Close view of a five-TMA-wide island (20 · 20 nm^2, $U_b = 1.54$ V, $I_t = 0.2$ nA) and (c) height profile along the line marked A−B revealing the different imaging contrast for adjacent TMA molecules and their intermolecular distances (*Z*-heights are given in a normalized scale and do not represent the absolute values).

bright features), which are associated with the individual TMA molecules, within the islands are markedly smaller (6.4 Å; cf. the height profile on Figure 3c) than the corresponding characteristic size of the flat adsorbed TMA identified in the low-temperature adlayer. The closer packing in the stripe phase is rationalized as a result from a bonding transition of adsorbed TMA. It is suggested that a reorientation of TMA from a flat-lying to an upright-standing conformation takes place as a result of carboxylate formation following deprotonation of TMA carboxyl groups due to the chemical activity of the copper substrate. The STM contour line along the islands reveal that the height of the upright species amounts to 1.3−1.5 Å, which does not reflect that expected from molecular geometry. This is rationalized by the fact that the STM topograph reflects the electronic structure of the surface. For example, in the case of 4-[*trans*-2-(pyrid-4-yl-vinyl)]benzoic acid on Cu(111), the upright-standing molecule, 12.3 Å in molecular geometry, only has a height of ∼1.4 Å in STM,[34] which was assigned to a poor electric conductance along the molecular axis. The second interesting feature of the room temperature phase is that the TMA molecules show exclusively spherical appearance in STM, independent of the bias voltage. Further studies reveal that under certain conditions the stripe phase can be transformed into a new one, in which TMA molecules have a clear triangular shape, signaling a flat-lying geometry. Thus the spherically shaped TMA observed by STM does not contradict an upright-standing geometry. Carboxylate formation is a typical finding at Cu surfaces, and analogous surface chemical bonds evolve upon thermal activation with simpler species containing a carboxyl group (e.g., benzoate/Cu(110),[35−38] acetate/Cu(110),[39] formate/Cu(100), and formate/Cu(110)[40,41]). Benzoic acid, reported as an exemplary compound with a carboxyl group for copper−carboxylate bond formation (see Perry et al.[37] and Frederick et al.[42] and references therein), initially adsorbs in a flat-lying benzoate configuration on Cu(110) and converts to the upright species close to saturation coverages, thus providing a reduced bonding area which allows more molecules to adsorb.[42] By contrast, studies of benzoate/Cu(111) system[37] evidence upright adsorption at very low coverages. With the present carboxylate, the molecule's anchoring at the substrate reflects the formation of a distinct chemisorption bond between substrate Cu atoms and the oxygen atoms of the carboxyl group. The corresponding gain in chemisorption energy with the upright geometry is expected to compensate for the loss of the π-bonding upon reorientation of the flat-lying species. For comparison, theoretical studies indicate a bonding energy of ∼2 eV for formate (HCOO) at Cu(100).[43,44]

Third, the STM data in Figure 3 reveal that each of the islands consists exclusively of an odd number of rows oriented in the stripe direction (we observed islands consisting of three, five, seven, or even nine TMA rows running parallel), where the molecules are topographically inequivalent (cf. the STM contour line in Figure 3c). We concentrate on the discussion of stripes with five row width. There, the very central row is always imaged more brightly. Furthermore, the topographic height of neighboring rows alternates, i.e., the second and fourth rows are imaged slightly darker. Finally, within any row, the individual TMA do not perfectly follow a line in the stripe direction. Rather, they are arranged in a zigzag mode, whereby every second molecule in the second and fourth rows is imaged with a slightly reduced height. The different imaging heights of adjacent molecules (either within a row or in adjacent rows) are presumably related to different bonding configurations of TMA molecules at the substrate: possibly through either one or two deprotonated carboxyl groups available for carboxylate formation in two different upright molecular orientations. Both calculations[43,44] and experimental evidence[35−37,39,41] indicate that upright carboxylates have a strong preference for the short-bridge site occupation, where a carbon atom lies midway between two next-neighbor copper surface atoms, with whom the oxygen atom forms chemical bonds.

In the case of trimesic acid, no experimental data or theoretical investigations concerning the carboxylate adsorption sites are available. However, our tentative adsorption scenario based on geometrical reasoning strongly favors a structural model of bidentate copper−carboxylate bonding where TMA can either be adsorbed through one carboxylate located at a short bridge site, or through two carboxylates, both centered at the

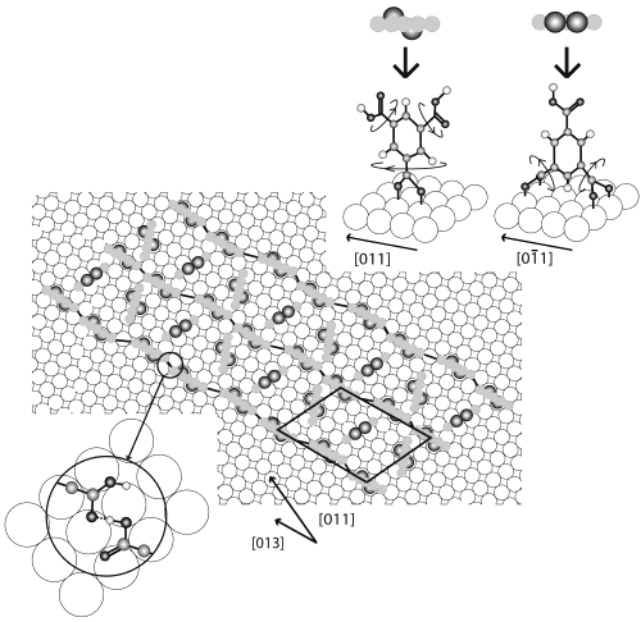

Figure 4. Tentative structural model for the striped supramolecular arrangement consisting of five TMA rows running parallel. The stripe orientation and the Cu(100) azimuth are indicated. Within a stripe-shaped island, molecules are represented schematically with an emphasis on the adsorption sites. In the upper right, two possible anchoring geometries of TMA-derived carboxylates are shown. The conformational rotation of carboxyl groups in respect to the C−C bond is assumed and shown by arrows. Oxygen atoms are shown in black, carbon atoms in light gray, and hydrogen atoms in white. In the lower left, a possible H-bonding geometry along the stripe orientation is indicated. The unit cell of the structure is marked.

short-bridge site and thus rotated in respect to the phenyl ring plane by 90°, with the molecule's center at a hollow site (a similar geometry was reported for phthalic anhydride adsorption on Cu(110)[45]). These configurations are shown in Figure 4. Preliminary investigations indicate that once the TMA molecule is bound in an upright-standing configuration, further deprotonation of the remaining carboxylic groups is delayed or requires higher thermal energies, since they are no longer in direct contact with the copper substrate. A tentative model for a stripe phase island consisting of five molecular rows is reproduced in Figure 4. This arrangement is believed to be stabilized by H-bond formation between the intact carboxyl groups within the first, third, and fifth rows in the direction of the island orientation (a similar weaving of molecules within the rows via hydrogen bonding is proposed for tartaric acid molecules adsorbed on Cu(110)[7]). TMA bound at short-bridge sites account for the zigzag arrangement in the odd-numbered rows. The second and the fourth rows, where STM revealed periodic changes in the imaging height, are believed to comprise two bonding configurations. In both cases, hydrogen bonding to the odd-numbered rows can be achieved when a ladder-type network is assumed. Hence, the TMA ordering in the stripe phase is presumably related to the formation of a supramolecular ladder-type structure. The edges of the ladders only consist of short bridge site adsorbed TMAs, while every second interlink within the ladder is a hollow-site adsorbed molecular species. By analogy, the one-dimensional islands of three TMA rows constitute single ladders, those of five TMA rows double ladders, and so forth. In our model, the hollow-site adsorbed TMA molecules are constrained in space by their four-point attachment to the surface via two carboxylate groups, which imparts the rigid and well-defined adsorption geometry. For short bridge site adsorbed TMA, we make use of the fact that carboxylates can freely rotate around the C−C bond (an analogy can be drawn with thiophene carboxylic acid adsorption on Cu(110),[46] where the rotation of the molecular plane is attributed to the intermolecular interaction) and thus the molecular plane (defined by the aromatic ring) can be rotated to optimize the hydrogen-bonding configuration. The different contrast in the STM images for the neighboring rows can be deduced directly from the structural model, where short bridge site adsorbed TMAs give brighter contrast than hollow-site adsorbed ones.

The stripe phase has no long-term stability at 300 K; at intermediate coverages, configurations with stabilities lasting up to several hours were observed. With longer periods or upon annealing to 400 K, the stripe phase is destabilized by free copper adatoms evaporated from the substrate steps. Eventually, well-defined complexes are formed. Preliminary results indicate that deprotonation of all carboxyl groups occurs and the TMA molecules change their orientation with respect to the substrate again to switch back to a flat-lying geometry forming metal−organic complexes with the copper adatoms. The nature of these complexes is currently under detailed investigation.

4. Conclusions

In conclusion, the self-assembly of trimesic acid molecules on a Cu(100) surface has been investigated by variable-temperature STM. We have identified two phases with distinct self-assembled supramolecular architectures, which can be rationalized by the subtle balance between adsorbate−substrate and intermolecular interactions. At low temperatures, π-bonding of flat-lying TMA to the substrate occurs. The molecules arrange in 2D islands where locally hydrogen-bonded honeycomb structures due to the carboxyl endgroups' dimerization are found. It is suggested that extended H-bond connected networks will be obtained at less reactive substrates or substrates with reduced surface potential energy corrugation. At room temperature, the catalytic activity of the copper substrate drives the deprotonation of carboxyl groups, which leads to an upright molecular adsorption geometry, where chemisorbed TMA molecules are anchored to the substrate through carboxylate formation. The upright TMA orders in striped islands, which are associated with H-bonded supramolecular ladders consisting of an odd number of TMA rows.

Acknowledgment. Financial support from the *Volkswagen-Stiftung* is gratefully acknowledged.

References and Notes

(1) Lindsey, J. S. *New J. Chem.* **1991**, *15*, 153.
(2) Whitesides, G. M.; Mathias, J. P.; Seto, C. T. *Science* **1991**, *254*, 1312.
(3) Lehn, J.-M. *Supramolecular Chemistry: Concepts and Perspectives*; VCH: Weinheim, 1995; Vol. 227.
(4) Philip, D.; Stoddart, J. F. *Angew. Chem., Int. Ed. Engl.* **1996**, *35*, 1154.
(5) Kawai, T.; Tanaka, H.; Nakagawa, T. *Surf. Sci.* **1997**, *386*, 124.
(6) Böhringer, M.; Morgenstern, K.; Schneider, W.-D.; Berndt, R.; Mauri, F.; Vita, A. d.; Car, R. *Phys. Rev. Lett.* **1999**, *83*, 324.
(7) Lorenzo, M. O.; Baddeley, C. J.; Muryn, C.; Raval, R. *Nature* **2000**, *404*, 376.
(8) Furukawa, M.; Tanaka, H.; Sugiura, K.; Sakata, Y.; Kawai, T. *Surf. Sci.* **2000**, *445*, L58.
(9) Barth, J. V.; Weckesser, J.; Cai, C.; Günter, P.; Bürgi, L.; Jeandupeux, O.; Kern, K. *Angew. Chem., Int. Ed. Eng.* **2000**, *39*, 1230.
(10) Barbosa, L. A. M. M.; Sautet, P. *J. Am. Chem. Soc.* **2001**, *123*, 6639.
(11) Weckesser, J.; Vita, A. D.; Barth, J. V.; Cai, C.; Kern, K. *Phys. Rev. Lett.* **2001**, *87*, 096101.
(12) *Introduction to Molecular Electronics*; Petty, M. C., Bryce, M. R., Bloor, D., Eds.; Oxford University Press: New York, 1995.

(13) Tour, J. M.; Kozaki, M.; Seminario, J. M. *J. Am. Chem. Soc.* **1998**, *120*, 8486.
(14) Chen, J.; Reed, M. A.; Rawlett, A. M.; Tour, J. M. *Science* **1999**, *286*, 1550.
(15) Prins, L. J.; Reinhoudt, D. N.; Timmerman, P. *Angew. Chem., Int. Ed. Eng.* **2001**, *40*, 2382.
(16) Duchamp, D. J.; Marsh, R. E. *Acta Crystallogr. Sect. B* **1969**, *25*, 5.
(17) Herbstein, F. H. *Top. Curr. Chem.* **1987**, *140*, 107.
(18) Herbstein, F. H. 1,3,5-Benzenetricarboxylic Acid (Trimesic Acid) and Some Analogues. In *Comprehensive Supramolecular Chemistry*; Atwood, J. L., MacNicol, D. D., Vögtle, F., Lehn, J.-M., Eds.; Pergamon: New York, 1996; Vol. 6; p 61.
(19) Kolotuchin, S. V.; Thiessen, P. A.; Fenlon, E. E.; Wilson, S. R.; Loweth, C. J.; Zimmerman, S. C. *Chem. Eur. J.* **1999**, *5*, 2537.
(20) Chatterjee, S.; Pedireddi, V. R.; Ranganathan, A.; Rao, C. N. R. *J. Mol. Struct.* **2000**, *520*, 107.
(21) Brune, H.; Röder, H.; Bromann, K.; Kern, K. *Thin Solid Films* **1995**, *264*, 230.
(22) IR and Mass Spectra. In *NIST Chemistry WebBook, NIST Standard Reference Database No. 6*; Linstrom, P. J., Mallard, W. G., Eds.; National Institute of Standards and Technology: Gaithersburg, MD, 2001; (http://webbook.nist.gov).
(23) Herbstein, F. H.; Kapon, M.; Maor, I.; Reisner, M. *Acta Crystallogr. B* **1981**, *37*, 136.
(24) Stöhr, J. *NEXAFS Spectroscopy*; Springer-Verlag:, 1991; Vol. 25.
(25) Hallmark, V. M.; Chiang, S.; Meinhardt, K.-P.; Hafner, K. *Phys. Rev. Lett.* **1993**, *70*, 3740.
(26) Chiang, S. *Chem. Rev.* **1997**, *97*, 1083.
(27) Lee, A. F.; Wilson, K.; Lambert, R. M.; Goldoni, A.; Baraldi, A.; Paolucci, G. *J. Phys. Chem. B* **2000**, *104*, 11729.
(28) Weckesser, J.; Barth, J. V.; Kern, K. *J. Chem. Phys.* **1999**, *10*, 5351.
(29) Sautet, P. *Chem. Rev.* **1997**, *97*, 1097.
(30) Lippel, P. H.; Wilson, R. J.; Miller, M. D.; Wöll, C.; Chiang, S. *Phys. Rev. Lett.* **1989**, *62*, 171.
(31) Seitsonen, A., private communication, 2001.
(32) Hydrogen Transfer: Experiment and Theory. In *Ber. Bunsen-Ges. Phys. Chem.*; Limbach, H.-H., Manz, J., Eds.; **1998**, *102*, 289.
(33) Barth, J. V. *Surf. Sci. Rep.* **2000**, *40*, 75.
(34) Weckesser, J., Ph.D. Thesis, Ecole Polytechnique Fédérale de Lausanne (EPFL), Switzerland, 2000.
(35) Frederick, B. G.; Ashton, M. R.; Richardson, N. V. *Surf. Sci.* **1993**, *292*, 33.
(36) Frederick, B. G.; Chen, Q.; Leibsle, F. M.; Lee, M. B.; Kitching, K. J.; Richardson, N. V. *Surf. Sci.* **1997**, *394*, 1.
(37) Perry, C. C.; Haq, S.; Frederick, B. G.; Richardson, N. V. *Surf. Sci.* **1998**, *409*, 512.
(38) Chen, Q.; Perry, C. C.; Frederik, B. G.; Murray, P. W.; Haq, S.; Richardson, N. V. *Surf. Sci.* **2000**, *446*, 63.
(39) Weiss, K.-U.; Dippel, R.; Schindler, K.-M.; Gardner, P.; Fritzsche, V.; Bradshaw, A. M. *Phys. Rev. Lett.* **1992**, *69*, 3196.
(40) Bowker, M.; Madix, R. J. *Surf. Sci.* **1981**, *102*, 542.
(41) Woodruff, D. P.; McConville, C. F.; Kilcoyne, A. L. D. *Surf. Sci.* **1988**, *201*, 228.
(42) Frederick, B. G.; Leibsle, F. M.; Haq, S.; Richardson, N. V. *Surf. Rev. Lett.* **1996**, *3*, 1523.
(43) Casarin, M.; Granozzi, G.; Sambi, M.; Tondello, E. *Surf. Sci.* **1994**, *307−309*, 95.
(44) Sambi, M.; Granozzi, G.; Casarin, M.; Rizzi, G. A.; Vittadini, A.; Caputi, L. S.; Chiarello, G. *Surf. Sci.* **1994**, *315*, 309.
(45) Haq, S.; Bainbridge, R. C.; Frederick, B. G.; Richardson, N. V. *J. Phys. Chem. B* **1998**, *102*, 8807.
(46) Frederick, B. G.; Chen, Q.; Barlow, S. M.; Condon, N. G.; Leibsle, F. M.; Richardson, N. V. *Surf. Sci.* **1996**, *352−354*, 238.